CCS Chemistry

RESEARCH ARTICLE

Received: Feb. 14, 2020 | Accepted: Mar. 5, 2020

Flat-Panel Laser Displays Based on Liquid Crystal Microlaser Arrays

Fa Feng Xu[1,2], Yong Jun Li[1], Yuanchao Lv[1], Haiyun Dong[1], Xianqing Lin[1], Kang Wang[1], Jiannian Yao[1,2] & Yong Sheng Zhao[1,2]*

[1]*Key Laboratory of Photochemistry, Institute of Chemistry, Chinese Academy of Sciences, Beijing 100190 (China),* [2]*University of Chinese Academy of Sciences, Beijing 100049 (China).*

**Corresponding author: yszhao@iccas.ac.cn*

Cite this: *CCS Chem.* **2020**, *2*, 369–375

Laser displays, benefiting from the characteristic merits of lasers, have led to the revolution of next-generation display technologies owing to their superior color expression. However, the acquisition of pixelated laser arrays as self-emissive panels for flat-panel laser displays remains challenging. Liquid crystal (LC) materials with excellent processability and optoelectronic properties offer considerable potential for the construction of highly ordered multicolor laser arrays. Here, we demonstrate flat-panel laser displays on LC microlaser pixel arrays through a microtemplate-assisted inkjet printing method. Individual organic red-green-blue (RGB) microlaser pixel arrays were obtained by doping dyes into LCs with photonic band edges to obtain single-mode RGB lasing, leading to a much broader color gamut, compared with the standard RGB color space. Then we acquired periodically patterned RGB pixel matrices by positioning LC microlasers precisely into highly ordered arrays, according to the well-organized geometry of the microtemplates. Subsequently, we demonstrated full-color flat-panel laser displays using the LC microlaser pixel matrices as self-emissive panels. These results provide valuable enlightenment for the construction of next-generation flat-panel laser display devices.

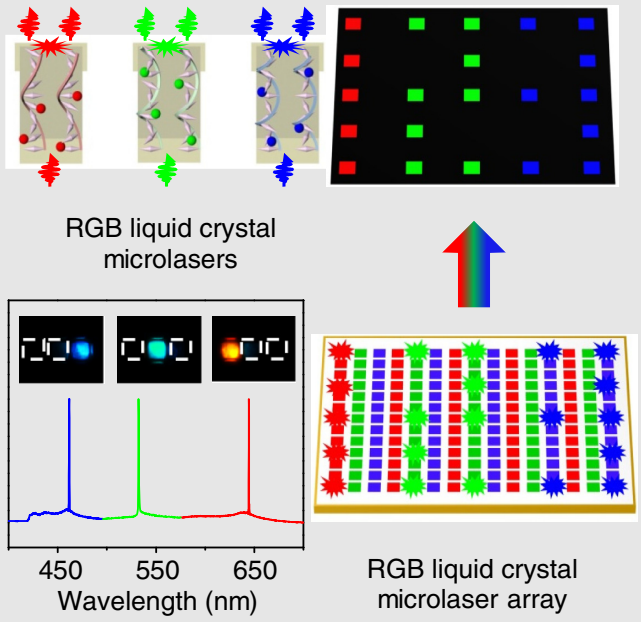

Keywords: **laser display, liquid crystal laser, laser array, full-color laser, single-mode laser, wide color gamut**

Introduction

Laser displays take advantage of high monochromaticity and brightness of laser emissions. They have emerged as revolutionary technologies in the display industries owing to their high saturation, high contrast ratio, and extensive achievable color gamut.[1–3] The requirement for laser displays in portable devices calls for appropriate self-emissive display panels. To this end, the development of pixelated structures is required, where each

DOI: 10.31635/ccschem.020.202000162
CCS Chem. **2020**, *2*, 369–375

microunit could realize laser emission and a collection of these lasers are well-arranged into periodic red-green-blue (RGB) arrays.[4–7] However, a universal fabrication technique for constructing such highly ordered emissive geometries is lacking and desires an urgent need.[8–10] Photolithography has been successfully applied in silicon-based photonics to produce patterned micro/nano-laser arrays.[11,12] In contrast, the acquisition of multicolor emissive units on a single chip remains challenging due to poor material compatibility.[13,14] Organic materials with excellent compatibility[15–17] permit their fabrication into multicolor lasers;[18–24] nevertheless, it is still difficult to pattern organic microlasers precisely into a pixelated RGB matrix on an identical substrate for the implementation of laser display panels.

Liquid crystals (LCs) have outstanding processability; thus, they have been exploited extensively for mass production of pixelated panels within flat-panel display fields, where the LCs in each pixel serve as passive polarization components to modulate the transmission of light.[25,26] Apart from these passive applications, LCs could also be utilized to achieve self-emissive lasers[27,28] for high-brightness and high-saturation displays in cases where they have been doped with luminescent dyes to generate self-assembled photonic crystal superstructures, acting as natural optical cavities.[29] More importantly, LC optical cavities could produce single-mode laser emissions inherently, owing to the periodically modulated refractive index.[30–32] The primary wavelengths of RGB single-mode LC lasers are located at the outer border of the chromaticity diagram to define the most extensive possible color gamut for vivid displays.[1] Therefore, it seems that LCs would be promising candidates for the fabrication of pixelated laser display panels based on the fusion of LC systems capable of lasing with mature panel production techniques. However, the realization of such panels has been impeded by the difficulties in fabricating miniaturized individual LC lasers and patterning them into periodic RGB pixel matrices.[33,34]

Herein, we proposed a strategy of microtemplate-assisted inkjet printing to construct full-color laser display panels composed of pixelated LC microlaser arrays. The polymeric microtemplates guided the positioning of LC microlasers precisely to give rise to ordered pixel arrays according to their well-organized geometry. We fabricated the RGB LC lasers by incorporating corresponding dyes into the respective LCs with distinct photonic band edges. Individual RGB display pixels consisting of adjacent three LC microlasers enabled tunable lasing across the full visible spectrum. Using the prepared LC microlaser pixel matrices as display panels, we achieved full-color laser displays. These results offer a robust approach to construct periodic microlaser pixel arrays and provide valuable insight into the development of next-generation flat-panel laser displays.

Experimental Method

Substrate preparation

The substrates, including indium tin oxide (ITO), glass, silicon, and magnesium fluoride (MgF_2), were cleaned in oxygen plasma for 5 min to produce hydrophilic surfaces, beneficial for the subsequent coating of polymeric films. MgF_2 wafers were selected as the substrates for the construction of display panels because of their low reflective index (1.38), able to reduce optical loss from the substrates, and lower the threshold of laser emissions.

Fabrication of polymeric microtemplates

We prepared polymeric microtemplates by etching polymeric films via electron beam lithography (EBL). The polymeric films were obtained by spin-coating a poly (methyl methacrylate) solution (20 wt %, in chlorobenzene) on the pretreated substrates at 1000 rpm for 1 min and baked on a heating stage at 180 °C for 5 min to eliminate the solvent. Then we carried out electron beam exposures by using an e-beam writer (ELPHY Quantum; Raith GmbH, Germany) at 30 kV with a beam current of 120 pA a beam-spot size of 3.0 nm, and a patterning dose of 0.5 mC/cm^2. Finally, the sample was immersed in the mixed solution of isopropyl alcohol and methyl isobutyl ketone (3:1) for 30 s. The microtemplates on the glass substrates, ITO, MgF_2, and silicon wafers were all obtained through the processes mentioned above. Notably, the microtemplates on the glass substrate were prepared with the assistance of a conductive adhesive, which was precoated on the polymeric film to eliminate charge effect during the EBL process.

Fabrication of LC microlasers

The LC-filled microunits were prepared by printing inks into the polymeric microtemplates through a GIX™ Microplotter™ II from SonoPlot Inc. (Middleton, WI, USA). The cholesteric LC inks (LC 1, LC 2, and LC 3) were prepared by dissolving 27 (9 wt %), 12 (4 wt %), and 5 mg (1.7 wt %) of the chiral dopant (S811) in the LC (I32-010E-425) solutions (300 mg), respectively. The ink solutions were imbibed into a hollow glass needle through capillary effect and sprayed into prefabricated microtemplates, assisted by ultrasonic vibration. By adjusting the ultrasonic vibration strength, an ink solution, perfectly filled microunits were acquired.

Fabrication of pixelated LC microlaser arrays

We prepared microunit laser arrays by printing emissive inks selectively into microtemplates at specific positions on the substrates. Then RGB emissive inks were obtained by dissolving 4.5 mg each of DCM, C30, and o-MSB in

DOI: 10.31635/ccschem.020.202000162
CCS Chem. **2020**, *2*, 369–375

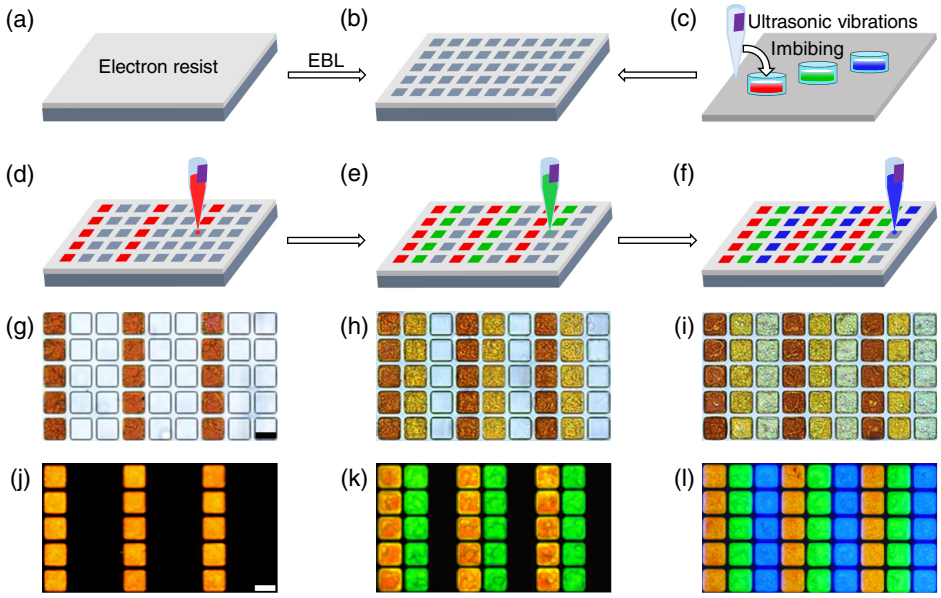

Figure 1 | *The fabrication of LC microlaser arrays. (a and b) Schematic illustration for the processing of polymeric microtemplates by EBL. (c–f) Schematic illustration of the microtemplate-assisted inkjet printing. (g–l) Bright-field and (j–l) PL images of printed pixel arrays. PL images were obtained under irradiation of UV light (330–380 nm). Scale bars are 50 μm.*

300 mg of LC solution (1.5 wt %). The three emissive inks were periodically deposited into the microtemplates by column to produce pixelated LC microlaser RGB arrays. The hollow glass needle was washed initially with dichloromethane to avoid ink contamination before the printing process.

Characterization of individual LC microlasers

The morphology of the polymeric microtemplates was examined by a step profiler (Bruker DektakXT; Beijing, China) and a contour graph (Bruker ContourGT-K1). The transmission and fluorescence spectra were measured by a UV–visible spectrometer (Perkin-Elmer Lambda 35; Shanghai, China) and a fluorescent spectrometer (Hitachi F-7000; Tokyo, Japan), respectively. We acquired bright-field and fluorescence microscopy images using an inverted fluorescence microscope (Nikon Ti-U; Beijing, China) by exciting the samples with halogen and mercury lamps, respectively. We carried out optically pumped lasing measurements for the individual pixels on a custom microphotoluminescence system. The excitation pulses (400 nm) were generated from the second harmonic of the fundamental output of a regenerative amplifier (Spectra Physics, 800 nm, 150 fs, 1 kHz), seeded with a mode-locked Ti:sapphire laser (Mai Tai, Spectra Physics, 800 nm, 150 fs, 80 MHz). We focused the excitation laser down to a 20 μm diameter spot through an objective lens (Nikon CFLU Plan, ×20, N.A. = 0.5) after filtering with a 720 nm short-pass filter. A neutral density filter was used to alter the power of the laser. After removing the excitation beam with a 420 nm long-pass filter, the emissions from the individual microunits were collected with the aid of the objective lens and analyzed by optical emission spectrometry (PDA 7000; Shimadzu Co. Ltd., Shanghai, China). A far-field photograph of the display panel was taken under the irradiation of a 400 nm laser with a built-in digital camera of a cellphone.

Results and Discussion

Fabrication of RGB LC microlaser pixel arrays

We prepared LC microlaser arrays by selectively printing cholesteric LC ink solutions into polymeric microtemplates at specific positions, according to the predesigned digital patterns. As schematically illustrated in Figure 1a and b, polymeric microtemplates were first fabricated by etching a flat film of photoresist polymethylmethacrylate with EBL, which was pre-spin-coated on an MgF_2 substrate. Then LC ink solutions were imbibed with a hollow glass needle through capillary effect and deposited into these microtemplates, assisted by ultrasonic vibration (Figure 1c–f). The as-fabricated microtemplates possessing columnar morphology (Supporting Information Figure S1) confined the deposited ink solutions tightly. The amount of deposited ink solutions was controlled precisely by adjusting the ultrasonic vibration strength to produce an ink solution that filled the microunits perfectly (Supporting Information Figure S2). The shape and size of the microunits were modulated rationally by

DOI: 10.31635/ccschem.020.202000162
CCS Chem. **2020**, *2*, 369–375

varying the corresponding structure parameters of the microtemplates (Supporting Information Figures S3 and S4). According to the well-organized geometry of the microtemplates, the fabricated microunits could be patterned into highly ordered arrays with dense packing density (Supporting Information Figure S5). Moreover, this microtemplate-assisted array fabrication method was suitable for most organic ink solutions (Supporting Information Figure S6) on a variety of substrates (Supporting Information Figure S7).

In the as-fabricated microunits, multidomain LC superstructures were obtained by introducing the chiral dopant into the LC host (Supporting Information Figure S8), which served as photonic crystal cavities to support laser oscillations at photonic band edges (Supporting Information Figure S9). The lasing wavelength could be altered over a wide range by doping various dyes into the LC inks with distinct band edges. Three laser dyes, 1,4-bis (2-methylstyryl)benzene (*o*-MSB), 7-(diethylamino)-3-(1-methyl-2-benzimidazolyl)coumarin (C30), and 4-(dicyanomethylene)-2-methyl-6-(4-dimethylaminostyryl)-4H-pyran (DCM), whose photoluminescence (PL) emissions localized in the blue, green, and red wavebands, respectively (Supporting Information Figure S10), were doped separately into the LC ink solutions. We performed printing of DCM-, C30-, and *o*-MSB-doped ink solutions sequentially into the microtemplates by column produced pixelated RGB microunit arrays (Figure 1g–i). The as-fabricated microunit arrays could extend to a large area (Supporting Information Figure S11), which was necessary for practical image display applications. Every three adjacent microunits along the row direction of the arrays functioned as an individual display pixel comprising RGB subpixels. Under UV light irradiation, these microscale pixels with uniform geometric shapes and independent forms emitted bright RGB fluorescence (Figure 1j–l), demonstrating the feasibility of the idea that these fabricated microunit arrays could serve as full-color panels for self-emissive laser displays.

Single-mode lasing from individual pixels

RGB lasing from the fabricated microunits was achieved with LC superstructures serving as photonic crystal cavities and embedded laser dyes providing optical gains, as depicted in Figure 2a. When the microunits were excited separately with a focused pulsed laser beam (400 nm, ~150 fs, and 1 kHz) in a custom microphotoluminescence system (Supporting Information Figure S12), we obtained modulated PL spectra at relatively low pump energy (<2.5 μJ cm^{-2}) with more intense emissions at the band edges than those inside the bandgaps of the LCs (Supporting Information Figure S13). Such unique modulation of PL emissions could be ascribed to the distribution of the density of optical states[35] and is beneficial for the generation of low-threshold lasing at

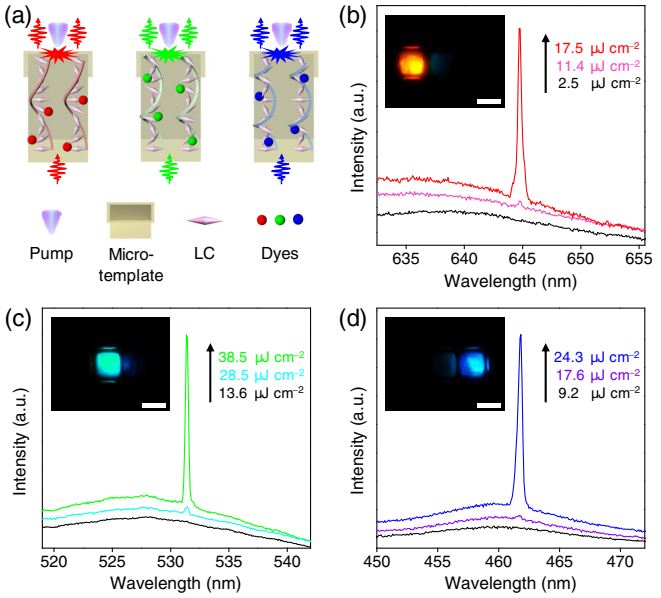

Figure 2 | *Single-mode lasing of an individual RGB pixel. (a) Sketch of individual RGB LC microlasers. (b–d) PL spectra of the red- (b), green- (c), and blue-emissive (d) micropixels under different pump fluences. Insets: Corresponding PL images. Scale bars are 20 μm.*

long-wavelength band edges of LCs.[36] With increasing pump fluence, the PL intensities of the RGB emissive microunits at ~644, ~531, and ~462 nm were amplified dramatically, respectively (Figure 2b–d). The lasing actions were confirmed after plotting the corresponding PL intensity as a function of the pump fluence and observing an exhibition of characteristic clear knee behavior at their respective thresholds of ~12.5, ~31.8, and ~17.2 μJ cm^{-2} (Supporting Information Figure S14). We obtained single-mode lasing emissions from the RGB microunits due to the spatially modulated refractive index in LC superstructures. We envisioned that the wavelengths of such RGB single-mode microlasers would be located at the outer border of the chromaticity diagram, which should define the most extensive possible color gamut for vivid displays.[1] We found that the full-width at half-maximum of the lasing modes were as narrow as 0.3–0.7 nm, affording ultrahigh spectral purity for high-saturation displays. Moreover, the lasing characteristics of these microunits were well maintained upon modulating their structural parameters, including thickness (Supporting Information Figure S15), edge length (Supporting Information Figure S16), and shape (Supporting Information Figure S17).

Full-color lasing in the pixel arrays

The multicolor lasing behavior of the microunits provided an opportunity to construct full-color emissive panels for laser displays by adding color. In this work, we evaluated

DOI: 10.31635/ccschem.020.202000162
CCS Chem. **2020**, *2*, 369–375

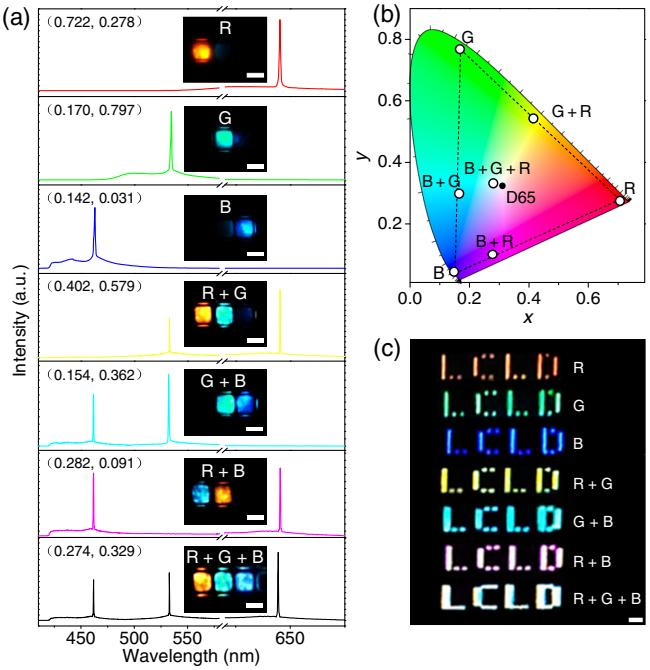

Figure 3 | *Full-color lasing combinations from RGB subpixels. (a) Lasing spectra of different combinations of RGB subpixels. Insets: Corresponding PL images and CIE1931 coordinates calculated from respective spectra. Scale bars are 20 μm. (b) Chromaticity distribution of the lasing peaks on the CIE1931 color diagram. The peaks were extracted from seven spectra in (a). (c) Far-field photograph of the "LCLD" patterns composed of different RGB pixel arrays. The photograph was captured by a built-in digital camera in a cell phone. Scale bar is 150 μm.*

the color expression based on the PL spectra of several subpixel combinations by selectively pumping different combinations in an individual RGB pixel. By so doing, we demonstrated monochromatic RGB lasing, simultaneous two-color lasing (R + G, G + B, R + B), and finally tri-color lasing (R + G + B) (Figure 3a). The chromaticity for these lasing spectra was calculated and plotted on the CIE1931 color diagram (Figure 3b). In this diagram, the chromaticity of the tri-color lasing (R + G + B) locates closely to the position of the CIE standard white illuminant D6537. The chromaticity of the primary RGB colors defined a triangle region, inside of which all colors could be obtained through mixing RGB colors in proper proportions, according to Grassmann's law.[37] After converting to a perceptually uniform color space, the triangle region covers obtained 196.6% perceptible colors, compared with the standard RGB space (Supporting Information Figure S18 and Tables S1 and S2), which suggested the existence of a broad color gamut. These results demonstrated the advantage of the LC microlaser arrays in realizing vivid displays with outstanding color fidelity.

In order to examine the far-field color rendering, which is a key feature of practical laser displays,[2,38] we prepared a range of LC microlaser arrays with the same pattern "LCLD" (acronym of "Liquid Crystal Laser Displays"). Then we took their far-field real-color photographs under laser irradiation. As depicted in Figure 3c, not only red, green, and blue "LCLD" patterns comprised the printed monochromatic microunits but also yellow, cyan, and magenta patterns composed of R + G, G + B, and R + B emissive microunits, respectively, were obtained in the far-field and were captured readily by the naked eyes. Furthermore, a rendered white-emissive pattern was acquired when the RGB microlaser array was exploited. These results demonstrated an experimental proof of concept for the construction of an LC microlaser array composed of full-color laser display panels.

Flat-panel laser displays with the pixelated panels

We carried out practical laser displays through selective pixels excitation at different positions[39] in the pixelated RGB arrays, since any given image was composed of a matrix of pixels. Various patterns and images were converted into their corresponding digital masks. Subsequently, the integral excitation was performed by manipulating a digital micromirror device with masks to reflect selectively, the excitation beam to light up specific pixels for picture displays (Figure 4a). Illustration in Figure 4b–d presents a 3 × 9 pixel array displaying red-, green-, and blue-emissive "L" characters by simultaneously exciting the microunits at specific positions matching the digital masks with distinct "L" patterns. Accordingly, large-scale image displays on the RGB microlaser pixel matrixes were generated by employing further large-sized digital masks with desired patterns. As an example, an image of the red-emissive dragon was presented on a centimeter-scale panel (1.2 cm in diagonal size, 123 × 144 micropixels, Figure 4e), validating the applicability of the fabricated microunit matrices as laser display panels for large-scale image displays. Moreover, programming the digital masks into more complicated pictures led to the display of colorful images; the image of a full-color facial makeup (Figure 4f) under precise excitation (Figure 4g) demonstrated a method of realizing colorful image displays. These results verified the notion that LC microlaser arrays could well be applied to serve as self-emissive, full-color panels for flat-panel laser displays.

Conclusion

We have demonstrated full-color laser display panels with RGB LC microlaser arrays fabricated through a microtemplate-assisted inkjet printing method. LC microlasers were well-positioned into a pixelated matrix, according to the geometry of the microtemplates, where every three adjacent RGB microlasers served as an

DOI: 10.31635/ccschem.020.202000162
CCS Chem. **2020**, *2*, 369–375

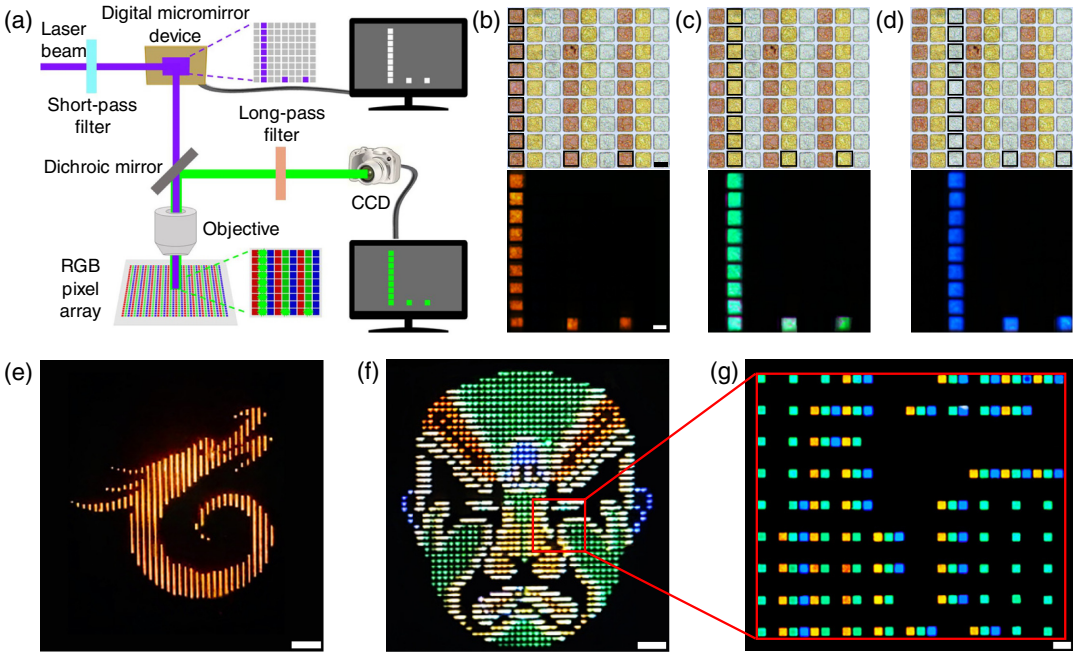

Figure 4 | *Full-color flat-panel laser displays. (a) The concept for flat-panel laser displays through selective excitations. A pulsed laser was introduced into a digital micromirror device, which reflected the laser beam to specific locations on the prefabricated panels. Colorful image displays could be realized by adopting different digital masks. (b–d) Bright-field (top) and PL (bottom) images of the prefabricated pixelated RGB arrays. The multicolor "L" could be obtained through exciting respective microunit combinations with different digital masks depicted as black squares in the top panels. Scale bars are 50 μm. (e, f) Images of laser display prototypes on an identical full-color panel (1.2 cm in diagonal size) with a 123 × 144 micropixel array. Scale bars are 1 mm. (g) High-magnification microscopy image of the selected area in (f). Scale bar is 100 μm.*

individual pixel. Laser emissions from display pixels were modulated to cover the full visible spectrum, which exhibited excellent color rendering features. Using large-scale LC microlaser pixel matrixes as display panels, we achieved full-color laser displays. These results are an inspiration for the construction of periodic multicolor laser arrays and open new avenues for creating high-performance flat-panel laser display and lighting devices.

Supporting Information

Supporting Information is available.

Conflict of Interest

There are no competing interests.

Acknowledgments

This work was supported financially by the Ministry of Science and Technology of China (no. 2017YFA0204502), the National Natural Science Foundation of China (grant nos. 21533013 and 21790364).

References

1. Chellappan, K. V.; Erden, E., Urey, H. Laser-Based Displays: A Review. *Appl. Opt.* **2010**, *49*, F79–F98.
2. Zhao, J.; Yan, Y.; Gao, Z.; Du, Y.; Dong, H.; Yao, J.; Zhao, Y. S. Full-color Laser Displays Based on Organic Printed Microlaser Arrays. *Nat. Commun.* **2019**, *10*, 870.
3. Neumann, A.; Wierer, J. J.; Davis, W.; Ohno, Y.; Brueck, S. R. J.; Tsao, J. Y. Four-Color Laser White Illuminant Demonstrating High Color-Rendering Quality. *Opt. Express* **2011**, *19*, A982–A990.
4. Müller, C. D.; Falcou, A.; Reckefuss, N.; Rojahn, M.; Wiederhirn, V.; Rudati, P.; Frohne, H.; Nuyken, O.; Becker, H.; Meerholz, K. Multi-Colour Organic Light-Emitting Displays by Solution Processing. *Nature* **2003**, *421*, 829–833.
5. Zheng, H.; Zheng, Y.; Liu, N.; Ai, N.; Wang, Q.; Wu, S.; Zhou, J.; Hu, D.; Yu, S.; Han, S.; Xu, W.; Luo, C.; Meng, Y.; Jiang, Z.; Chen, Y.; Li, D.; Huang, F.; Wang, J.; Peng, J.; Cao, Y. All-solution Processed Polymer Light-Emitting Diode Displays. *Nat. Commun.* **2013**, *4*, 1971.
6. Kim, T.-H.; Cho, K.-S.; Lee, E. K.; Lee, S. J.; Chae, J.; Kim, J. W.; Kim, D. H.; Kwon, J.-Y.; Amaratunga, G.; Lee, S. Y.; Choi, B. L.; Kuk, Y.; Kim, J. M.; Kim, K. Full-Colour Quantum Dot Displays Fabricated by Transfer Printing. *Nat. Photon.* **2011**, *5*, 176–182.

DOI: 10.31635/ccschem.020.202000162
CCS Chem. **2020**, *2*, 369–375

7. Choi, M. K.; Yang, J.; Kang, K.; Kim, D. C.; Choi, C.; Park, C.; Kim, S. J.; Chae, S. I.; Kim, T. H.; Kim, J. H.; Hyeon, T.; Kim, D. H. Wearable Red-Green-Blue Quantum Dot Light-Emitting Diode Array using High-Resolution Intaglio Transfer Printing. *Nat. Commun.* **2015**, *6*, 7149.
8. Briseno, A. L.; Mannsfeld, S. C.; Ling, M. M.; Liu, S.; Tseng, R. J.; Reese, C.; Roberts, M. E.; Yang, Y.; Wudl, F.; Bao, Z. Patterning Organic Single-Crystal Transistor Arrays. *Nature* **2006**, *444*, 913–917.
9. Feng, J.; Jiang, X. Y.; Yan, X. X.; Wu, Y. C.; Su, B.; Fu, H. B.; Yao, J.; Jiang, L. "Capillary-Bridge Lithography" for Patterning Organic Crystals Toward Mode-Tunable Microlaser Arrays. *Adv. Mater.* **2017**, *29*, 1603652.
10. Zhang, L.; Liu, H.; Zhao, Y.; Sun, X.; Wen, Y.; Guo, Y.; Gao, X.; Di, C. A.; Yu, G.; Liu, Y. Inkjet Printing High-Resolution, Large-Area Graphene Patterns by Coffee-Ring Lithography. *Adv. Mater.* **2012**, *24*, 436–440.
11. Wang, Z.; Tian, B.; Pantouvaki, M.; Guo, W.; Absil, P.; Campenhout, J. V.; Merckling, C.; Thourhout, D. V. Room-temperature InP Distributed Feedback Laser Array Directly Grown on Silicon. *Nat. Photon.* **2015**, *9*, 837–842.
12. Behzadirad, M.; Nami, M.; Wostbrock, N.; Kouhpanji, M. R. Z.; Feezell, D. F.; Brueck, S. R. J.; Busani, T. Scalable Top-Down Approach Tailored by Interferometric Lithography to Achieve Large-Area Single-Mode GaN Nanowire Laser Arrays on Sapphire Substrate. *ACS Nano* **2018**, *12*, 2373–2380.
13. Chen, R.; Tran, T.-T. D.; Ng, K. W.; Ko, W. S.; Chuang, L. C.; Sedgwick, F. G.; Chang-Hasnain, C. Nanolasers Grown on Silicon. *Nat. Photon.* **2011**, *5*, 170–175.
14. Fan, F., Turkdogan, S., Liu, Z., Shelhammer, D.; Ning, C. Z. A monolithic White Laser. *Nat. Nanotechnol.* **2015**, *10*, 796–803.
15. Clark, J. & Lanzani, G. Organic Photonics for Communications. *Nat. Photon.* **2010**, *4*, 438–446.
16. Koos, C.; Vorreau, P.; Vallaitis, T.; Dumon, P.; Bogaerts, W.; Baets, R.; Esembeson, B.; Biaggio, I.; Michinobu, T.; Diederich, F.; Freude, W.; Leuthold, J. All-Optical High-Speed Signal Processing with Silicon–Organic Hybrid Slot Waveguides. *Nat. Photon.* **2009**, *3*, 216–219.
17. Zhang, C.; Zou, C.-L.; Zhao, Y.; Dong, C.-H.; Wei, C.; Wang, H.; Liu, Y.; Guo, G.-C.; Yao, J.; Zhao, Y. S. Organic Printed Photonics: From Microring Lasers to Integrated Circuits. *Sci. Adv.* **2015**, *1*, e1500257.
18. Kuehne, A. J. C. & Gather, M. C. Organic Lasers: Recent Developments on Materials, Device Geometries, and Fabrication Techniques. *Chem. Rev.* **2016**, *116*, 12823–12864.
19. Berggren, M., Dodabalapur, A., Slusher, R. E. & Bao, Z. Light Amplification in Organic Thin Films Using Cascade Energy Transfer. *Nature* **1997**, *389*, 466–469.
20. Cerdán, L.; Enciso, E.; Martín, V.; Bañuelos, J.; López-Arbeloa, I.; Costela, A.; García-Moreno, I. FRET-Assisted Laser Emission in Colloidal Suspensions of Dye-doped Latex Nanoparticles. *Nat. Photon.* **2012**, *6*, 621–626.
21. Lv, Y.; Li, Y. J.; Li, J.; Yan, Y.; Yao, J.; Zhao, Y. S. All-Color Subwavelength Output of Organic Flexible Microlasers. *J. Am. Chem. Soc.* **2017**, *139*, 11329–11332.
22. Ta, V. D.; Yang, S. C.; Wang, Y.; Gao, Y.; He, T. C.; Chen, R.; Demir, H. V.; Sun, H. D. Multicolor Lasing Prints. *Appl. Phys. Lett.* **2015**, *107*, 221103.
23. Ha, N. Y.; Jeong, S. M.; Nishimura, S.; Suzaki, G.; Ishikawa, K.; Takezoe, H. Simultaneous Red, Green, and Blue Lasing Emissions in a Single-Pitched Cholesteric Liquid-Crystal System. *Adv. Mater.* **2008**, *20*, 2503–2507.
24. Dong, H.; Zhang, C.; Liu, Y.; Yan, Y.; Hu, F.; Zhao, Y. S. Organic Microcrystal Vibronic Lasers with Full-Spectrum Tunable Output Beyond the Franck-Condon Principle. *Angew. Chem. Int. Ed.* **2018**, *57*, 3108–3112.
25. Schadt, M. Liquid Crystal Materials and Liquid Crystal Displays. *Annu. Rev. Mater. Sci.* **1997**, *27*, 305–379.
26. Hikmet, R. A. M.; Kemperman, H. Electrically Switchable Mirrors and Optical Components made from Liquid-Crystal Gels. *Nature* **1998**, *392*, 476–479.
27. Coles, H. & Morris, S. Liquid-Crystal Lasers. *Nat. Photon.* **2010**, 4, 676–685.
28. Hands, P. J. W.; Gardiner, D.; Morris, S. M.; Mowatt, C.; Wilkinson, T. D.; Coles, H. J. Band-Edge and Random Lasing in Paintable Liquid Crystal Emulsions. *Appl. Phys. Lett.* **2011**, *98*, 141102.
29. Cao, W., Munoz, A., Palffy-Muhoray, P.; Taheri, B. Lasing in a Three-Dimensional Photonic Crystal of the Liquid Crystal Blue Phase II. *Nat. Mater.* **2002**, *1*, 111–113.
30. Criante, L., Lucchetta, D. E., Vita, F., Castagna, R.; Simoni, F. Distributed Feedback All-Organic Microlaser Based on Holographic Polymer Dispersed Liquid Crystals. *Appl. Phys. Lett.* **2009**, *94*, 111114.
31. Strangi, G.; Barna, V.; Caputo, R.; Luca, A. D.; Versace, C.; Scaramuzza, N.; Umeton, C.; Bartolino, R.; Price, G. N. Color-Tunable Organic Microcavity Laser Array Using Distributed Feedback. *Phys. Rev. Lett.* **2005**, *94*, 063903.
32. Lee, S. S., Kim, J. B., Kim, Y. H.; Kim, S.-H. Wavelength-Tunable and Shape-Reconfigurable Photonic Capsule Resonators Containing Cholesteric Liquid Crystals. *Sci. Adv.* **2018**, *4*, eaat8276.
33. Morris, S. M.; Hands, P. J. W.; Findeisen-Tandel, S.; Cole, R. H.; Wilkinson, T. D.; Coles, H. J. Polychromatic Liquid Crystal Laser Arrays Towards Display Applications. *Opt. Express* **2008**, *16*, 18827–18837.
34. Woltman, S. J. & Crawford, G. P. Patterned Liquid-Crystal Laser Film for Multi-Dimensional Multi-Color Emissive Film Technology. *J. Soc. Inf. Disp.* **2007**, *15*, 559–564.
35. Mavrogordatos, T. K.; Morris, S. M.; Castles, F.; Hands, P. J. W.; Ford, A. D.; Coles, H. J.; Wilkinson, T. D. Density of Photon States in Dye-Doped Chiral Nematic Liquid Crystal Cells in the Presence of Losses and Gain. *Phys. Rev. E* **2012**, *86*, 011705.
36. Liu, Y. J.; Sun, X. W.; Shum, P.; Li, H. P.; Mi, J.; Ji, W.; Zhang, X. H. Low-Threshold and Narrow-Linewidth Lasing from Dye-Doped Holographic Polymer-Dispersed Liquid Crystal Transmission Gratings. *Appl. Phys. Lett.* **2006**, *88*, 061107.
37. Luo, Z., Chen, Y.; Wu, S.-T. Wide Color Gamut LCD with a Quantum Dot Backlight. *Opt. Express* **2013**, *21*, 26269–26284.
38. Arsenault, A. C., Puzzo, D. P.,Manners, I.; Ozin, G. A. Photonic-Crystal Fullcolour Displays. *Nat. Photon.* **2007**, *1*, 468–472.
39. Deng, R.; Qin, F.; Chen, R.; Huang, W.; Hong, M.; Liu, X. Temporal Full-Colour Tuning Through Non-Steady-State Upconversion. *Nat. Nanotechnol.* **2015**, *10*, 237–242.

DOI: 10.31635/ccschem.020.202000162
CCS Chem. **2020**, *2*, 369–375